Article

Not peer-reviewed version

Trypsin vs. Papain: What Is the Best Digestive for Hippocampal Triculture Preparation?

Ivan Andreevich Tumozov , Valentina Nikolaevna Mal`tseva , Sergei Alexandrovich Maiorov , Artem Mikhailovich Kosenkov , Sergei Gennadevich Gaidin *

Posted Date: 25 November 2024

doi: 10.20944/preprints202411.1853.v1

Keywords: microglia; triculture; papain; CDr20; intracellular Ca^{2+} concentration; Iba1; ATP

Article

Trypsin vs. Papain: What Is the Best Digestive for Hippocampal Triculture Preparation?

Ivan A. Tumozov, Valentina N. Mal`tseva, Sergei A. Maiorov, Artem M. Kosenkov and Sergei G. Gaidin *

Federal Research Center "Pushchino Scientific Center for Biological Research of the Russian Academy of Sciences", Institute of Cell Biophysics of the Russian Academy of Sciences, 142290 Pushchino, Russian Federation;

* Correspondence: sergeigaidin@pbcras.ru

Abstract: Microglia, accounting for 5-15 % of total brain cells, is the essential population of glial cells in the cultures for modeling neuroinflammation in vitro. However, microglia proliferation is poor in the neuron-glial cultures. Here, we studied the population composition of rat hippocampal neu-ron-glial cell cultures prepared using papain (PAP-cultures) and trypsin (TRY-cultures) as prote-olytic enzymes for cell isolation. We have found that the microglia percentage in PAP-cultures was higher than in TRY-cultures. Microglia in PAP-cultures are predominantly polarized, while bushy morphology was more characterized for TRY-cultures. We have also studied the effects of the combination of TGFβ+MCSF+cholesterol, which should enhance microglia proliferation, on the population composition and microglia morphology. These factors increase the microglia number both in PAP- and TRY-cultures (to 25-30 % of the total number of cells) and promote the appearance of ameboid microglia characterized by high mobility. However, the significant appearance of ameboid microglia was observed already at the early stages of cultivation (2 DIV) in TRY-cultures while in PAP-cultures the described transformation was observed at 7DIV. Thus, our results demonstrate that papain is a more suitable proteolytic enzyme for preparing mixed hippocampal neuron-glial with a higher percentage of heterogenous microglia and functional neurons and astrocytes (tricultures).

Keywords: microglia; triculture; papain; CDr20; intracellular Ca^{2+} concentration; Iba1; ATP

1. Introduction

According to modern neurobiology paradigms, microglia is one of the main populations of glial cells in the mammalian brain. These cells function as resident brain macrophages and play a crucial role in neuroinflammatory processes [1]. Through their involvement in synaptic pruning (the elimination of excess synapses), microglia also serve as key regulators of synaptic plasticity [2]. The microglial population exhibits inherent heterogeneity, further amplified under pathological conditions due to phenotypic transformations [1]. Primary microglia cell cultures [3] or immortalized microglia-like cell lines [4] are a convenient and common object for in vitro neuroinflammation research. However, modeling comprehensive inflammatory responses necessitates intercellular interactions among diverse cell types [3]. To overcome this limitation, approaches are being developed to obtain co-cultures of separately grown populations of brain cells [5]. Although this approach makes it possible to vary the experimental design flexibly, namely choose the moment of addition of one cell population to another, the number of cells introduced, and pretreatment of one of the groups of cells with various test compounds, it is not without disadvantages. In addition to methodological difficulties in obtaining pure cell cultures of a particular population of brain cells and their different maturation periods, often requiring mixing of cells of different passages (or even from different animals), the absence of microenvironment in pure neuronal, microglial or astrocytic cultures, as well as the manipulations aimed to "purification," such as the addition of cytosine arabinoside in the case of neuronal cultures [6–8], or prolonged intense shaking in the case of astrocytic cultures [9], affect the phenotype of cells in the obtained cultures.

 doi:10.20944/preprints202411.1853.v1

Mixed tricultures in which the formation of closed, self-sufficient neuron-glial networks occurs and cells, including microglia, proliferate and mature in a more in vivo approximate microenvironment can be proposed as a solution to this problem. However, established protocols for mixed neuron-glial cultures utilizing trypsin for extracellular matrix degradation and Neurobasal medium+B27 Supplement combination as a culture medium typically result in limited microglial proliferation [10]. The addition of growth factors has been proposed to increase the amount of microglia in mixed neuron-glial cultures, but similar works are isolated [10–12].

Papain is often used as a digestive agent during the preparation of primary microglia cultures [5,13]. Although both papain and trypsin are proteolytic enzymes, the first belongs to cysteine proteases, while the latter is a serine protease. This difference means that hydrolysis of polypeptide sequences mediated by trypsin and papain occurs at different sites. Despite the long history of using these proteases during brain cell culture preparation, their effects were compared only in several studies [14,15] and only in the context of neurons. Based on these facts, we have decided to test how papain affects the functional state and population composition of the cultures, particularly the amount of microglia.

In this investigation, we examined how papain utilization for extracellular matrix degradation affects the population composition of mixed rat hippocampal neuron-glial cultures (PAP-cultures). Our findings demonstrate that papain use promotes increased microglial populations compared to trypsin-prepared cultures (TRY-cultures) without significant alterations in astrocyte and neuron quantities. Additionally, we observed that microglia in PAP-cultures predominantly exhibit polarized morphology, whereas TRY-cultures display predominantly bushy microglial morphology.

2. Materials and Methods

2.1. Preparation of Cell Cultures

The hippocampi of newborn male Wistar rats (P0-2) were used to prepare cell cultures. The brain extracted after decapitation was placed in a Versene ice-cold solution, and the hippocampus was separated. Then, hippocampal tissue was cut into small fragments with scissors. Afterward, the Versene solution was replaced with a 1% trypsin solution (in Versene solution) or a 0.8% papain solution (in Versene solution). As in our numerous previous studies [16–21], incubation with trypsin was carried out at 37 ^{0}C for 10 minutes under constant shaking (500 rpm) in a thermoshaker. In the case of papain, the incubation time was 25 minutes, as ineffective matrix dissociation occurred with less incubation time, and the cell suspension contained large amounts of debris. Hippocampal fragments treated with these enzymes were washed twice with cold Neurobasal medium and then gently triturated in 1 mL of Neurobasal medium with an automatic pipette (1 mL tip was used). Undissociated tissue fragments were carefully removed by pipette, and the obtained suspension was centrifuged for 3 minutes at 2000 rpm. The resulting cell pellet was resuspended in Neurobasal medium to obtain a suspension with the cell density of 700,000 cells/ml. The Neubauer counting chamber was used to evaluate the quantity of cells before the dilution. Glass cylinders with an inner diameter of 6 mm were used to concentrate the cells on the confined surface. The cylinders were set on round cover glasses of 24 mm diameter placed in sterile Petri dishes of 35 mm diameter and pre-coated to improve cell adhesion with polyethyleneimine solution (1 mg/ml) for 50 minutes, followed by overnight drying. 100 µl of suspension was poured into each cylinder. Petri dishes with cylinders filled with cell suspension were covered with lids and carefully transferred to a CO_2 incubator for 40 minutes for cell attachment. After that, the cylinders were carefully removed using tweezers, and 2 mL of the culture medium consisting of Neurobasal medium, 2% serum-free B27 supplement, 0.5 mM glutamine, and penicillin/streptomycin (100 U/ml) was added to the dishes. Since postnatal cells were used to prepare cultures, sterile sodium chloride solution was added to Neurobasal medium to achieve a final NaCl concentration in the medium of 4 g/L. The cells were grown in a CO_2 incubator at 37 ^{0}C, 95% humidity, and 5% CO_2 in the atmosphere. Cells were taken for experiments on the 2nd, 7th, and 14th days of culture (2, 7, and 14 DIV, respectively). In the case of cultures grown using

 doi:10.20944/preprints202411.1853.v1

additionally introduced factors (TGFβ 2 ng/mL, MCSF 5 ng/mL, cholesterol 100 μg/mL), the addition of compounds to the culture medium was carried out immediately after removal of the cylinders.

2.2. Fluorescent Microscopy

Fluorescence microscopy was used to evaluate the population composition of cell cultures and the physiological activity of cells. Identification of neurons and glial cells was carried out based on calcium response (an increase of intracellular Ca^{2+} concentration ($[Ca^{2+}]_i$)) to the addition of potassium chloride (35 mM) and adenosine triphosphate (ATP, 10 μM), respectively. For this purpose, the cells were stained with a fluorescent Ca^{2+}-sensitive probe FluoriCa-8 AM (Fluo-8 AM analog). The probe staining and all subsequent experiments were performed in Hank's balanced salt solution (HBSS) of the following composition: 136 mM NaCl, 3 mM KCl, 0.8 mM $MgSO_4$, 1.25 mM KH_2PO_4, 0.35 mM Na_2HPO_4, 1.4 mM $CaCl_2$, glucose10 mM; HEPES 10 mM, pH=7,35. FluoriCa-8 was loaded at a temperature of 28°C for 40 minutes, after which the cultures were washed twice with HBSS and washed again 10 minutes later to allow the unesterified dye to leave the cells. The final concentration of FluoriCa-8 in the working solution was 5 μM. After washing, the coverslips with cell cultures were mounted in a microscopic chamber and placed on an inverted epifluorescence microscope Leica 6000 DMI, equipped with Leica IL-6000 illuminator (mercury lamp) and Hamamatsu 9100C CCD camera. L5 filter cube with BP 480/40 excitation filter, a dichroic mirror 505 nm, and BP 527/30 emission filter was used for excitation and emission detection of FluoriCa-8. The short-term addition of KCl and ATP and the subsequent wash-out were carried out in a flow of HBSS using a special perfusion system (flow rate 10 mL/min).

A fluorogenic substrate of UDP-glucoronosyl transferase [22] CDr20 Microglia Stain (CDr20) was used to identify microglia cells. Since the enzyme is specific for microglia cells, other cell types do not transform the dye in culture. TX2 filter cube with BP 560/40 excitation filter, a dichroic mirror 595 nm and BP 645/75 emission filter was used to excite and record the CDr20 fluorescence. CDr20 application was performed in HBSS flow, and dynamics of the staining were registered with a frame rate of 1 frame per 5 seconds. A double-stranded DNA-binding fluorescent dye Hoechst 33342 at a concentration of 5 μg/mL was used to visualize the nuclei to further count the total number of cells in the culture. The cells were stained with the dye for 10 minutes and then washed with HBSS. An external filter BP387/15 and Fura-2 filter cube with 72100bs dichroic mirror and HQ 540/50m emission filter were used to excite and collect the Hoechst 33342 emission. In calcium imaging experiments, where more than one dye was not required, the fluorescent ratiometric Ca^{2+}-sensitive probe Fura-2 AM was used to assess changes in $[Ca^{2+}]_i$. Loading of cells with Fura-2 (3 μM) was carried out under conditions similar to those of FluoriCa-8 loading. Fura-2 cube, the characteristics of which are given above, was used to excite and record the emission.

2.3. Immunocytochemical Staining

Immunocytochemical staining was used to identify neurons, astrocytes, and microglia in rat hippocampal cell cultures, as well as assess the presence of glutamatergic and GABAergic synapses on neurons. Cell cultures removed from the CO_2 incubator were washed three times with phosphate-buffered saline (PBS; pH=7.35) and then fixed with a 4% solution of freshly prepared paraformaldehyde for 20 minutes. The paraformaldehyde solution was prepared by dissolving the weighed amount in PBS with constant stirring at 70°C in a fume hood until a clear solution was obtained. After cooling the solution, undissolved aggregates were removed by filtration through a polyethersulfone membrane with a pore size of 0.22 μm. Cells were washed from paraformaldehyde with ice-cold PBS three times. Goat serum (10% in PBS) was used to block the non-specific binding of secondary antibodies. Simultaneously with blocking, cell membrane permeabilization was performed using Triton X-100 at a concentration of 0.1% for intracellular antigens. In contrast, a milder detergent, Tween 20, was used for surface antigens at a concentration of 0.2%. Goat serum and detergents were dissolved in PBS. Cells were incubated with a blocking solution containing the corresponding detergent at room temperature for 30 minutes, after which cells were washed once with 1% goat serum solution (in PBS) for 5 minutes. Primary antibodies were dissolved in the same

 doi:10.20944/preprints202411.1853.v1

solution. The dilutions of primary antibodies are indicated in the corresponding figure legends. Cells were incubated with primary antibodies at +4°C for 12 hours, followed by triple washing with PBS (each PBS incubation interval lasted 5 minutes). Then, cell cultures were incubated with goat secondary antibodies dissolved in PBS for 90 minutes in the dark at room temperature, followed by triple washing with PBS. Secondary antibodies used were goat anti-mouse immunoglobulins (conjugated with Alexa Fluor 647) and anti-rabbit immunoglobulins (conjugated with Alexa Fluor 488). Secondary antibodies were diluted 1:300. To visualize cell nuclei, cells were incubated with Hoechst 33342 (5 μg/ml in PBS) for 10 minutes and washed twice with PBS.

The distribution of antibodies to synaptic markers vGAT and vGluT2 was visualized using a Leica TCS SP5 confocal microscope. Neuron-specific enolase (NSE) served as a neuronal marker. Goat antibodies to mouse immunoglobulins (conjugated to Alexa Fluor 647), rabbit immunoglobulins (conjugated to Alexa Fluor 555), and guinea pig immunoglobulins (conjugated to Alexa Fluor 488) were used as secondary antibodies. The dilution of all secondary antibodies was 1:300. Dilutions of primary antibodies are indicated in the figure legends. He-Ne lasers with excitation bands 633 and 543 nm and argon laser with excitation band 488 nm were used for excitation. Scanning was performed in Z-stack mode, with each dye being scanned in a separate stack with one active laser to avoid overlap of excitation/emission spectra.

2.4. Data Analysis

Image processing was performed using ImageJ and LAS AF Lite software. The total number of cells in the field of view was counted in ImageJ using the Analyze Particles software option. Images of Hoechst 33342-stained cell nuclei were used for counting. Due to the peculiarities of cell cultures, consisting of the formation of conglomerates, cells in these structures were counted manually to avoid artefacts caused by the peculiarities of the Analyze Particles algorithm. OriginLab Pro 2021 software was used for plotting graphs. Statistical analysis of data and diagram construction were performed using GraphPad Prism 8. Data are presented as mean±SD.

2.5. Substances

The reagents that were used in the experiments are listed below. 1) *Sigma-Aldrich, Saint Louis, MO, USA:* Poly(ethyleneimine) solution (Cat. no. P3143), TWEEN® 20 (Cat. no. P1379), Paraformaldehyde (P6148); L-Glutamine (Cat. no. G8540), Anti-SLC32A1 (N-terminal) antibody (anti-vGAT) produced in rabbit (Cat. no. SAB2700790). 2) *Life Technologies, Grand Island, NY, USA*: B-27 supplement (Cat. no. 17504044), Trypsin 2.5% (Cat. no. 15090046). 3) *Molecular Probes, Eugene, OR, USA*: Fura-2 AM (Cat. no. F1221); 4) *Cayman Chemical, Ann Arbor, MI, USA*: Bicuculline (Cat. no. 11727). 5) *Paneco, Moscow, Russian Federation*: Neurobasal medium (H333), penicilin-streptomycin (A063); 6) *Abcam, Cambridge, UK*: Goat Anti-Mouse IgG H&L (Alexa Fluor® 647) (Cat. no. ab150115), Goat Anti-Rabbit IgG H&L (Alexa Fluor® 555) (Cat. no. ab150078), Goat Anti-Guinea pig IgG H&L (Alexa Fluor® 488) (Cat. no. ab150185), Goat serum New Zeland origin (Cat. no. 16210072). 7) *HyTest, Moscow, Russian Federation*: mouse monoclonal antibodies to neuron-specific enolase (Cat. no. 4N6), mouse monoclonal antibodies to glial fibrillar acidic protein (Cat. no. 4G25); 8) *Lumiprobe, Moscow, Russian Federation*: FluoriCa-8 AM (Fluo-8 AM analog) (Cat. no. 3391), LumiCell CDr20 Microglia Stain (Cat. no. 3570). 9) *Sci-Store, Moscow, Russian Federation*: active human macrophage colony stimulating factor (MCSF) (Cat. no. PSG280). 10) *Cloud-Clone Corp, Wuhan, China*: Polyclonal Antibody to Allograft Inflammatory Factor 1 (AIF1) (Cat. no PAC288Ra01), Active Transforming Growth Factor Beta 1 (Cat. no. APA124Ra01). 11) *CDH Ltd., New Delhi, India*: Cholesterol (Cat. no. 043011). 12) *LOBA Chemie, Mumbai, India*: Papain Extra Pure (Cat. no. 05110). 13) *Amresco LLC, Solon, OH, USA*: Triton X-100 (Cat. no. Am-O694). 14) *Synaptic Systems GmbH, Goettingen, Germany*: Guinea pig polyclonal anti-VGLUT2 antibody (Cat. no. 135 404).

3. Results

3.1. Comparison of Population Composition of Cultures Prepared Using Trypsin and Papain

 doi:10.20944/preprints202411.1853.v1

To determine the population composition of cell cultures obtained using trypsin (TRY-culture) and papain (PAP-culture), we initially used an immunocytochemical staining method using primary antibodies to neuron-specific enolase (NSE), glial fibrillar acid protein (GFAP) and Iba1, which are markers of neurons, astrocytes, and microglia, respectively. We evaluated the number of cells in 2, 7, and 14 DIV cultures. Because GFAP is a structural filament protein accumulating in the processes [23] and on the second day of cultivation, as our experiments have shown (see Supplementary, Figure S1), only a portion of astrocytes have processes (processes are removed during enzymatic treatment and subsequent mechanical dissociation during culture preparation), we hypothesized that counting cells based on immunocytochemical staining data, especially astrocytes, on the second day of cultivation might lead to incorrect results. In this regard, we present counting results only for 7 and 14 DIV cultures (Figure 1).

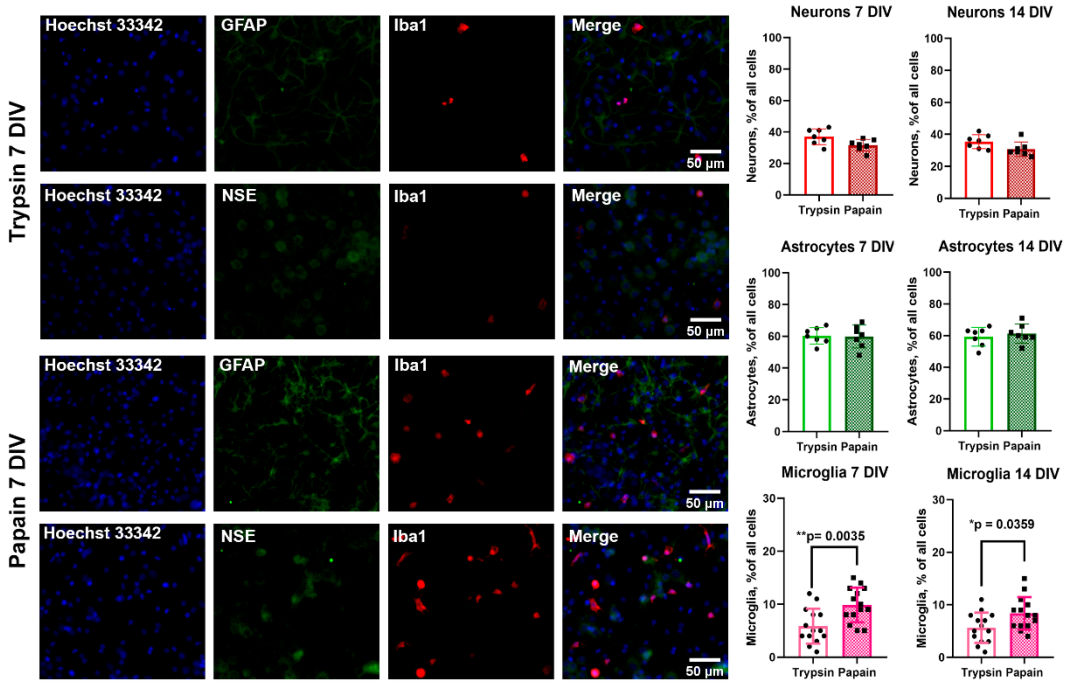

Figure 1. On the left: representative images of 7DIV neuron-glial rat hippocampal cultures stained with antibodies to neuronal marker NSE (neuron-specific enolase, dilution 1:200), a marker of astrocytes GFAP (glial fibrillar acid protein, dilution 1:300), and calcium-binding protein Iba1 (ionized calcium-binding molecule 1, microglia marker; dilution 1:200). On the right: the diagrams showing the number of neurons, astrocytes, and microglia in 7 and 14 DIV TRY- and PAP-cultures. Unpaired t-test.

Immunostaining shows that the difference between the number of neurons and astrocytes in TRY- and PAP-cultures is negligible both in 7 and 14 DIV cultures. In turn, the amount of $Iba1^+$ microglia (cells stained with anti-Iba1 antibodies) differed significantly.

To confirm the immunocytochemical staining data and indirectly assess physiological activity, we further characterized the number of cells of three populations by fluorescent imaging. As noted in the materials and methods section, potassium chloride and ATP applications were used to identify neurons and glial cells. As shown in our previous works [16,17], potassium chloride causes an increase in $[Ca^{2+}]_i$ (Figure 2A, red arrows; Figure 2B) only in neurons. This is explained by the fact that increasing the concentration of potassium ions in the external environment changes the electrochemical gradient of this ion in cells, resulting in reduced K^+ efflux from cells, which provides membrane potential hyperpolarization, thereby causing depolarization. Depolarization leads to the opening in neurons of voltage-gated sodium and calcium channels [17] followed by secretion of glutamate (the primary excitatory neurotransmitter), which activates ionotropic glutamate receptors (AMPA, NMDA and kainate receptors) mediating secondary influx of sodium and calcium ions

 doi:10.20944/preprints202411.1853.v1

through them. In turn, the secondary influx enhances depolarization and causes the opening of more voltage-gated calcium channels. Thus, the influx of calcium ions through the glutamate receptors and voltage-gated calcium channels during primary and secondary depolarization causes an increase in $[Ca^{2+}]_i$ in neurons presented in Figure 2B. Besides participating in energy metabolism inside cells, ATP acts as a messenger secreted into the external environment that affects purinergic receptors of the P_2X and P_2Y families [24,25]. These receptors are located in large numbers on the cell membrane of glial cells, while the membrane density and repertoire of these receptors are lower on neurons. Neurons are more characterized by P_2X family receptors, which are ligand-gated cation channels. These receptors are activated by higher ATP concentrations compared to P_2Y receptors [26], reaching 1 mM in some subtypes. We used a concentration of 10 μM, which is sufficient to activate various subtypes of P_2Y and P_2X receptors. P_2Y receptors are metabotropic G-protein-coupled receptors. The biphasic increase in cytosolic Ca^{2+} concentration during ATP application observed in the figure is mainly due to P_2Y_1, P_2Y_2, P_2Y_4, P_2Y_6, and P_2Y_{11} receptors coupled with the Gq protein. Activation of these receptor subtypes through the Gq-subunit leads to activation of the intracellular enzyme phospholipase C [27], enhancing the accumulation of inositol-3-phosphate (IP_3), which in turn activates IP_3 receptors of the endoplasmic reticulum, through which accumulated Ca^{2+} ions are released into the cytosol. The depletion of intracellular calcium stores in the reticulum causes the opening of STIM-Orai channels responsible for replenishing reticulum calcium stores. These processes cause the change in $[Ca^{2+}]_i$ during ATP application. Such processes certainly occur in neurons as well; however, due to the above-noted difference in receptor population composition and more powerful calcium clearance mechanisms providing calcium ion efflux from the cytosol to prevent calcium overload, a response similar to that in glial cells is not observed in these cells.

Thus, as part of the described approach, neurons in cultures were identified by the response to KCl, and glial cells by the response to ATP (Figure 2A, B). Since two populations of glial cells in hippocampal cultures capable of responding to ATP are astrocytes and microglia [25] (oligodendrocytes do not proliferate under the culture conditions used [28]), we used vital dye CDr20 to identify microglia cells. Figure 2 shows an example of staining of 7 DIV PAP-cultures. Experimentally, taking into account the recommendations of the developers [22] and manufacturers, we have determined that the most optimal for staining in terms of signal-to-noise ratio in our conditions is the working dye concentration of 80 nM (see Supplementary Figure S2). However, microglial staining was noted even at lower concentrations. According to CDr20 staining, ATP-responding $CDr20^+$ cells were considered microglia, while $CDr20^-$ cells responding to ATP were considered astrocytes. It should be noted that the patterns of responses to ATP in microglia and astrocytes differ (Figure 2C), which can be an additional criterion for the identification of these cell populations. Using calcium response patterns for KCl and ATP and the presence of CDr20 staining, we evaluated the number of neurons, astrocytes, and microglial cells in rat hippocampal PAP- and TRY-culture. Figure 2D shows that, as with immunocytochemical staining, the amount of microglia in PAP-cultures is higher than in TRY-cultures. A significant difference was noted in the case of 2, 7 DIV, 14 DIV cultures.

It can be concluded that according to two different methods of evaluating the population composition, the number of microglia cells in 7 DIV and 14 DIV PAP-cultures significantly exceeds the amount of microglia in TRY-cultures, while differences in the number of neurons and astrocytes were not significant. Moreover, the number of microglia on the 7th day of cultivation increases compared to the second day, and this difference is most characteristic of cultures prepared using papain. Consequently, microglia in cultures are capable of proliferation even within the standard protocol of preparation and cultivation of neuron-glial cultures.

 doi:10.20944/preprints202411.1853.v1

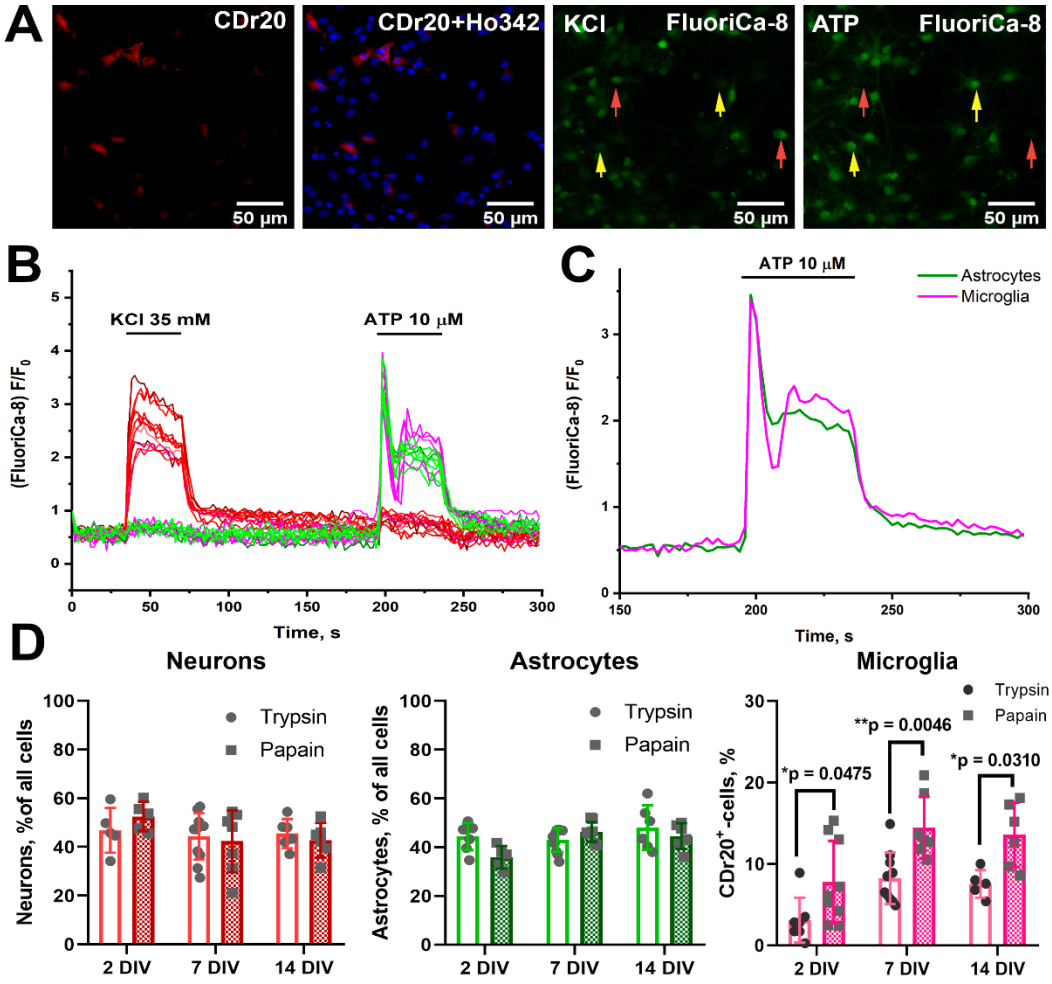

Figure 2. (***A***) Representative images of the rat hippocampal 7 DIV PAP-culture region. Cell cultures were stained with a fluorescent Ca^{2+}-sensitive FluoriCa-8 probe and vital microglia dye CDr20. Nuclei were stained with Hoechst 33342. In the case of FluoriCa-8, images corresponding to the time of KCl (35 mM) application with bright neurons and the time of ATP (10 μM) application with bright glial cells are shown. Representative neurons and glial cells are marked with red and yellow arrows, respectively. (***B***) Curves reflecting $[Ca^{2+}]_i$ changes in neurons (red curves), astrocytes (green curves), and microglia cells (purple curves) during KCl and ATP application. (***C***) Averaged astrocyte and microglia responses to ATP application. (***D***) Diagrams showing the number of neurons, astrocytes, and microglia in 2, 7, and 14 DIV cultures obtained using trypsin (columns without pouring) and papain (hatched columns). One-way ANOVA followed by Sidak`s multiple comparisons test.

3.2. Papain Does Not Affect the Synaptogenesis and Maturation of Neuronal Networks

Synaptogenesis and maturation processes occur in neuronal networks in cultures, as in the intact brain. The effect of papain use on the state of neuronal networks in the obtained cultures is controversial: on the one hand, in the case of papain, there is a large survival rate of neurons [14,29]; on the other hand, papain affects the morphology of soma, the length of axons, which can affect neurotransmission [15]. We did not note significant differences in the structures of emerging networks in PAP-cultures compared to TRY-cultures (Figure 1, Supplementary Figure S3), and we found slightly higher neuronal content in PAP-cultures on the second day of culture (Figure 2), although this difference was not significant in our experiments. However, the presence of neurons in cultures does not mean the presence of functional networks, so our further efforts were concentrated on testing functionality.

As is known, in neuronal networks between inhibition and excitation processes there is a fine balance (E/I balance) where inhibition prevails over excitation [30]. This balance is maintained

 doi:10.20944/preprints202411.1853.v1

through regulation of the activity of excitatory glutamatergic and inhibitory GABAergic neurons. The presence of glutamatergic and GABAergic synapses, whose selective markers are vesicular transporters of glutamate and GABA (vGluT2 [31] and vGAT [32], respectively), can be considered an indirect confirmation of network formation by these neuronal subtypes. Figure 3A shows a representative image of 14 DIV rat hippocampal PAP-neuron-glial culture stained with antibodies to vGAT and vGluT2. We used an antibody to the neuronal marker neuron-specific enolase (NSE) to visualize neurons. As shown in Figure 3A, PAP-cultures demonstrate the formation of dense neuronal networks with developed GABAergic and glutamatergic innervation. Similar morphology and innervation were demonstrated using the same antibodies in our previous work [19], where trypsin was used to digest the extracellular matrix during cell isolation.

We used the calcium imaging method to confirm the presence of mature functional networks connecting hundreds of neurons in hippocampal PAP-cultures. As noted above, the E/I balance concept implies the prevalence of inhibition over excitation. GABAergic inhibition is realized through the effect of GABA secreted by GABAergic neurons on $GABA_A$ and $GABA_B$ receptors ($GABA_A$Rs and $GABA_B$Rs, respectively). Suppression of $GABA_A$R-mediated inhibition using selective antagonists, such as bicuculline, leads to the prevalence of excitation over inhibition, excessive neuronal excitation, and subsequent generation of epileptiform activity, manifesting as regular oscillations of intracellular Ca^{2+} concentration in neurons [20]. Figure 3B shows the dynamics of $[Ca^{2+}]_i$ changes in representative neurons (red curves) of 14 DIV PAP-culture. The presence of regular $[Ca^{2+}]_i$ oscillations occurring quasi-synchronously in multiple neurons in the field of view in the presence of $GABA_A$R antagonists may indicate the presence of a closed neuronal network with developed GABAergic innervation.

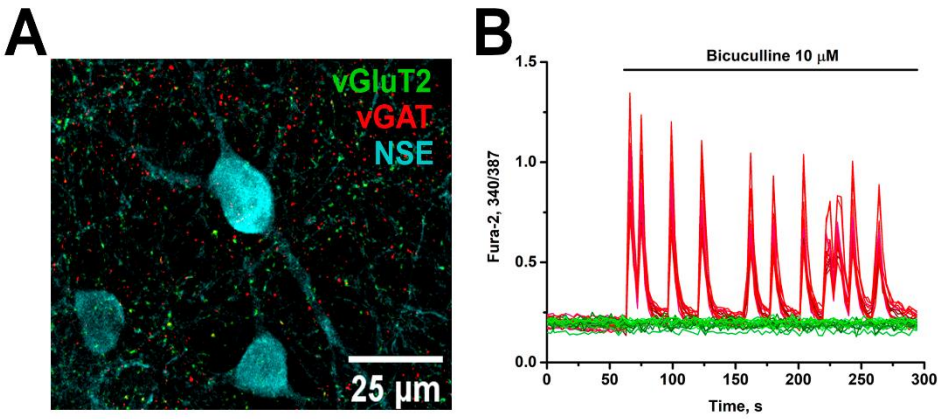

Figure 3. (***A***) Representative image of immunocytochemical staining of 14 DIV PAP-culture with antibodies against glutamatergic synapse marker (vGluT2, dilution 1:500), GABAergic synapse marker (vGAT, dilution 1:500), and neuronal marker, neuron-specific enolase (NSE, dilution 1: 200) (***B***) Induction of regular high-amplitude $[Ca^{2+}]_i$ oscillations in neurons (red curves) of PAP-cultures after application of GABAAR antagonist, bicuculline (10 µM). A ratiometric fluorescent Ca^{2+}-sensitive Fura-2 probe was used to evaluate the $[Ca^{2+}]_i$ changes. Green curves correspond to glial cells.

3.3. Microglia Morphology in PAP-Cultures Differs from Microglia Morphology in TRY-Cultures

Using dye CDr20, we found that microglia in the obtained neuron-glial cultures differed in shape and staining profile. Since significant differences in microglial quantity and minimal deviations in this parameter were noted above for 7DIV cultures, further experiments were continued with cultures of this age. As for the morphology of microglia cells in cultures, like other researchers [33], we noted the presence of polarized microglia, which has mainly two opposite-sided processes (Figure 4A, upper row, magenta arrows), as well as microglia with several processes diverging in different directions, which we defined as bushy (Figure 4A, upper row, yellow arrows). Similar morphological profiles were detected using anti-Iba1 antibodies (Figure 4A, lower row). Notably, the amount of polarized microglia was significantly higher in PAP-cultures than in TRY-cultures (Figure 4B).

 doi:10.20944/preprints202411.1853.v1

We also found interesting features of the loading/transformation kinetics of the fluorogenic UDP-glucoronosyl transferase substrate, CDr20, in the microglia cells of the two phenotypes. To evaluate loading kinetics, we performed staining with continuous fluorescence recording. The curves showing changes in CDr20 fluorescence in representative polarized (pink curves) and bushy microglial cells (red curves) are presented in Figure 4C. As a parameter most accurately highlighting the difference in cell loading kinetics patterns, we chose the time to reach 50% of maximum fluorescence intensity (half-rise time). As shown in the diagram in Figure 4D, the half-rise time is significantly higher in polarized microglia. Consequently, dye transformation occurs significantly faster in bushy microglia. Such differences in transformation kinetics of the fluorogenic UDP-glucuronosyl transferase substrate may indicate, for example, a greater quantity or activity of this enzyme in bushy microglial cells.

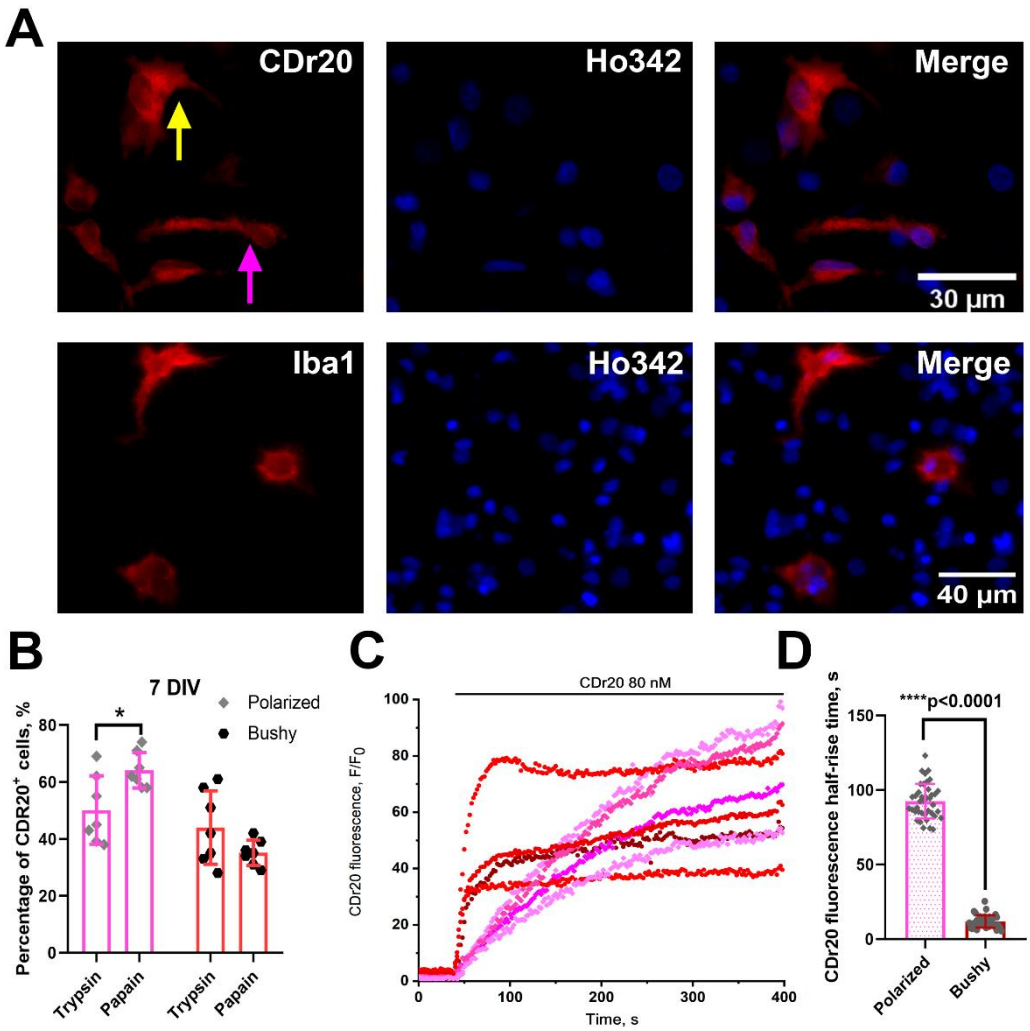

Figure 4. (***A***) Representative enlarged images of microglia in 7DIV PAP-cultures. Top row: CDr20⁺ microglia; bottom row: cultures stained with antibodies to Iba1. (***B***) Diagram showing the amount of polarized and bushy microglia in 7 DIV TRY- and PAP-cultures. Two-Way ANOVA followed by Sidak`s multiple comparison test. (***C***) Transformation kinetics of the fluorogenic UDP-glucoronosyl transferase substrate, CDr20 (microglia marker), in polarized (purple curves) and bushy (red curves) microglia. (***D***) A diagram reflecting differences in time to reach 50% of the maximum intensity of CDr20 fluorescence (half-rise time) in polarized and ameboid microglia. Unpaired t-test.

Thus, the use of papain for hippocampal tissue processing promotes the preservation and proliferation in the neuron-glial culture of microglia with a predominantly polarized form.

 doi:10.20944/preprints202411.1853.v1

3.4. Effect of the Combination of TGFβ+MCSF+Cholesterol Factors on the Population Composition of PAP- and TRY-Cultures Obtained Using Papain and Trypsin.

The work published earlier demonstrated [10] that the amount of Iba-1$^+$ microglia in neuron-glial culture can be increased by adding the following combination of factors to the culture medium: TGFβ (2 ng/mL), IL-34 (100 ng/mL) and cholesterol (100 μg/mL). In our experiments, the IL-34 had no significant effect on the amount of Iba-1$^+$ microglia, which may be due to the use of hippocampal cells. Therefore, given the similarity of the action of IL-34 and macrophage-colony stimulating factor (MCSF) [34], we made an appropriate replacement. Thus, in our experiments, we introduced the following factors into the culture medium during the preparation of neuron-glial cultures: TGFβ (2 ng/mL), MCSF (5 ng/mL) and cholesterol (100 μg/mL). To compare the population composition of cultures grown with the addition of this combination of compounds, we used above-mentioned calcium imaging approach with FluoriCa-8 staining followed by addition of KCl, ATP and CDr20 loading.

TGFβ+MCSF+cholesterol results in an increase in the amount of microglia in TRY-cultures, so it was decided to study how this combination of compounds would affect the amount of microglia in PAP-cultures. The addition of factors was carried out during the preparation of hippocampal cell cultures, whereas the population composition was evaluated, as in the case of the previous series of experiments, in 2 DIV and 7 DIV cultures. Figure 5 shows representative images of 7 DIV cell cultures grown using this combination of factors.

Preprints.org (www.preprints.org) | NOT PEER-REVIEWED | Posted: 25 November 2024 doi:10.20944/preprints202411.1853.v1

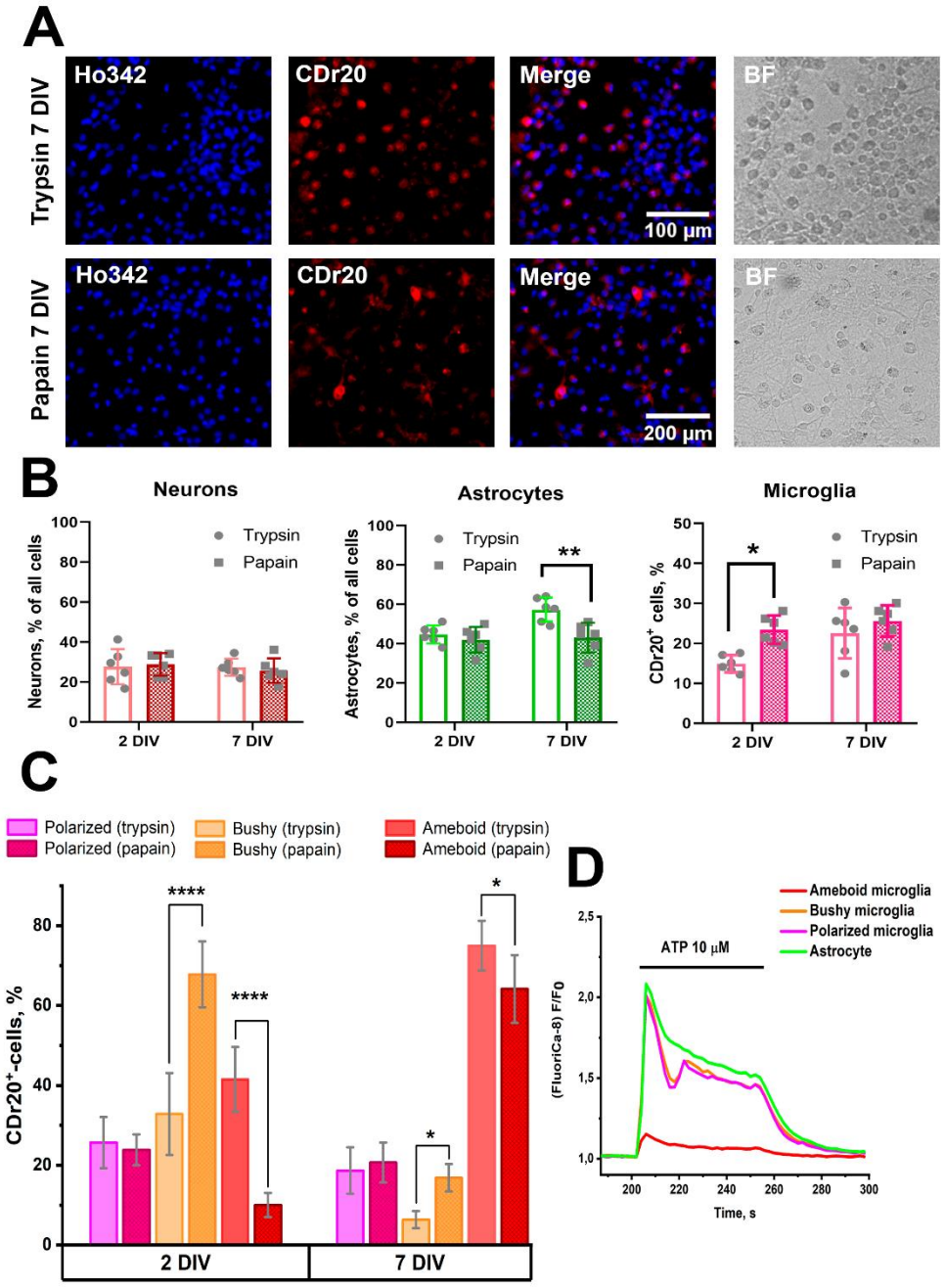

Figure 5. (***A***) Hippocampal TRY- and PAP-cultures grown in medium with addition of TGFβ+ MCSF+cholesterol. Cultures were stained with a specific microglia marker, CDr20, as well as nuclei dye, Hoechst 33342. Additionally, images of the same area of culture in transmitted light (BF) are presented. (***B, C***) Diagrams showing the population composition of TRY- and PAP-cultures (***B***) and the microglia morphology (***C***) in 2 DIV and 7 DIV cultures grown in the presence of TGFβ+MCSF+cholesterol. In Diagram B, the PAP-cultures correspond to hatched columns. Two-way ANOVA followed by Sidak`s (***B***) or Tukey`s (***C***) multiple comparison test. (***D***) Averaged curves showing $[Ca^{2+}]_i$ changes in astrocytes and microglia cells of different phenotype during ATP application (10 μM).

As shown in Figure 5, the combination of factors contributes to an increase in the amount of microglia 2 DIV and 7 DIV cultures compared to cultures grown without the factors (Figure 2), both in the case of TRY-cultures and in the case of PAP-cultures. It should be noted that the morphology of microglia in the presence of TGFβ+ MCSF+cholesterol differs from that of microglial cells shown in Figure 2. In this case, both microphotographs with CDr20 distribution and transmitted light images

 doi:10.20944/preprints202411.1853.v1

show a large number of process-free round cells, which were not almost observed in the case of cultures grown without factors (Supplementary, Figure S3). This microglia cells have been designated by us as a separate group – ameboid microglia. In the case of PAP-cultures, in addition to ameboid microglia, microglial cells with processes can be observed, indicating the heterogeneous population of this cell type. At the same time, as follows from the diagram in Figure 5, the number of neurons in TRY- and PAP-cultures varies insignificantly in 2 DIV and 7 DIV cultures. An interesting fact is that in the case of TRY-cultures, phenotype change (prevalence of ameboid microglia) is already observed on the second day of culture (Figure 5C), as there is a significant decrease in bushy count and an increase in ameboid microglia count compared to PAP cultures. Ameboid microglia as opposed to polarized and bushy was also found to have low-amplitude response to ATP application (Figure 5D, orange curve).

Thus, it can be concluded that the combination TGFβ+MCSF+cholesterol factors results in both an increase in the amount of microglia in cultures and its phenotypic changes, and in the case of TRY-cultures, the phenotype change of a significant part of microglia occurs almost after the culture preparation.

4. Discussion

In this work, we assessed the effects of trypsin and papain, used as enzymes for extracellular matrix dissociation, on the population composition of hippocampal cell cultures of newborn rats. According to the available conflicting literary data, the use of papain leads, on the one hand, to an increase in the number of neurons in cultures [14,29], whereas on the other hand, their morphology and probably network activity change [15]. In our experiments, we found that although the number of neurons in the first days of cultivation was slightly higher with papain, during further cultivation, their number did not significantly differ from cultures isolated using trypsin (Figures 1 and 2). Our data do not contradict literary in the context of population composition, as we noted a slightly larger number of neurons in PAP-cultures in early culture, whereas further offset of differences in neuronal count and the absence of pronounced changes in neuronal network morphology in our experiments may be due to differences in culture conditions and the subject of study used. Using two different evaluation techniques, we have found that the number of microglia cells in PAP-cultures is significantly different from the amount of microglia in TRY-cultures. It is known from literary data that papain is used as a proteolytic enzyme in the preparation of primary microglia cultures from the brain of both neonatal and adult animals [5,13], while assessment of its effect on microglial quantity in mixed neuron-glial cultures for developing a convenient model for neuroinflammation research apparently has not been conducted previously [4].

Although, depending on the microglia counting technique used, its number in our experiments varied almost twice, the differences between PAP- and TRY-cultures were still reliable. Iba1 is a classic microglia marker used in a variety of neuroinflammatory studies [35]. However, according to a number of studies, its expression may vary depending on experimental conditions, and some researchers consider it a marker of active microglia [35,36]. Moreover, the existence of Iba1- microglial populations in the brain [37–39], particularly in the hippocampus [37], has been previously reported. The selectivity of the UDP-glucuronosyl transferase fluorogenic substrate, CDr20, for microglial cells, has been demonstrated both in vitro and in vivo [22]. It can be assumed that CDr20 can stain both $Iba1^+$ and $Iba1^-$ microglia. This assumption would explain the greater number of $CDr20^+$ cells than $Iba1^+$ microglia in cultures. In this regard, we hypothesized that in the case of mixed cultures, where microglia have a microenvironment consisting of neurons and astrocytes, Iba1 is an unreliable marker for assessing the total number of microglia. In future studies using more constitutive microglial markers, we plan to evaluate the ratio of $CDr20^+$, $Iba1^+$, and $Iba1^-$ microglia and the possible overlap of these populations. Although the repertoire of microglial markers is quite extensive and includes many membrane-bound and cytosolic proteins, HEXb, TMEM119, and P_2Y_{12} are considered constitutive, microglia-selective, and species-nonspecific [40,41]. However, for the latter two, expression changes depending on conditions have recently been demonstrated [42].

 doi:10.20944/preprints202411.1853.v1

The difference we found in CDr20 transformation kinetics between different microglia phenotypes can have two explanations: cells of different phenotypes differ in enzyme activity/expression or rate of fluorogenic substrate penetration into the cytosol. Regarding the level of expression, recently published work notes that UDP-glucoronosyl transferase, due to stable expression under various conditions, can act as a universal marker of microglia, and the gene encoding it as a housekeeping gene [41], so differences in the rate of CDr20 penetration can be considered as the most likely explanation for the observed effect. Thus, dye transformation dynamics can be a criterion for phenotypic classification of microglia cells in vitro. In addition, the presence of ATP-induced $[Ca^{2+}]_i$ increase may be an additional criterion in this case. In the case of a combination of factors, the analog of which in earlier work was used to increase microglia proliferation in mixed neuron-glial cultures [10,11], we observed the appearance of a large amount of ameboid microglia characterized by a low-amplitude response to ATP application. Round amoeboid shape and changes in ATP response pattern can be considered manifestations of reactivity [43,44]. Changes in purinoreceptor expression profile during microglial activation, particularly decreased P_2Y_{12} receptor expression and increased P_2X_7 receptor expression [45], which require more than 1 mM ATP for activation, were noted in other authors' works, which may explain the decreased microglial sensitivity to ATP. Hence, microglia in cultures grown with TGFβ+MCSF+cholesterol can be considered predominantly activated. Indirect evidence of microglia reactivity is its mobility, as seen in our experiment with mechanical culture damage presented in Figure 6. Two days after scratching, in the case of cultures incubated with the combination of TGFb+MCSF+cholesterol factors, migration of amoeboid $Iba1^+$ microglia to the damaged area was observed (Figure 6, bottom row). Such a phenomenon was not observed in cultures grown according to the standard protocol. Thus, a combination of features, including ameboid form, motility, significant proliferation, and low-amplitude ATP-induced Ca^{2+} response, suggests that TGFb+MCSF+cholesterol cause microglia activation in mixed neuron-glial hippocampal cultures. It is worth noting that the kinetics of CDr20 transformation in ameboid microglia cells had a similar pattern to the kinetics of bushy microglia transformation, so we do not show it separately in the figures.

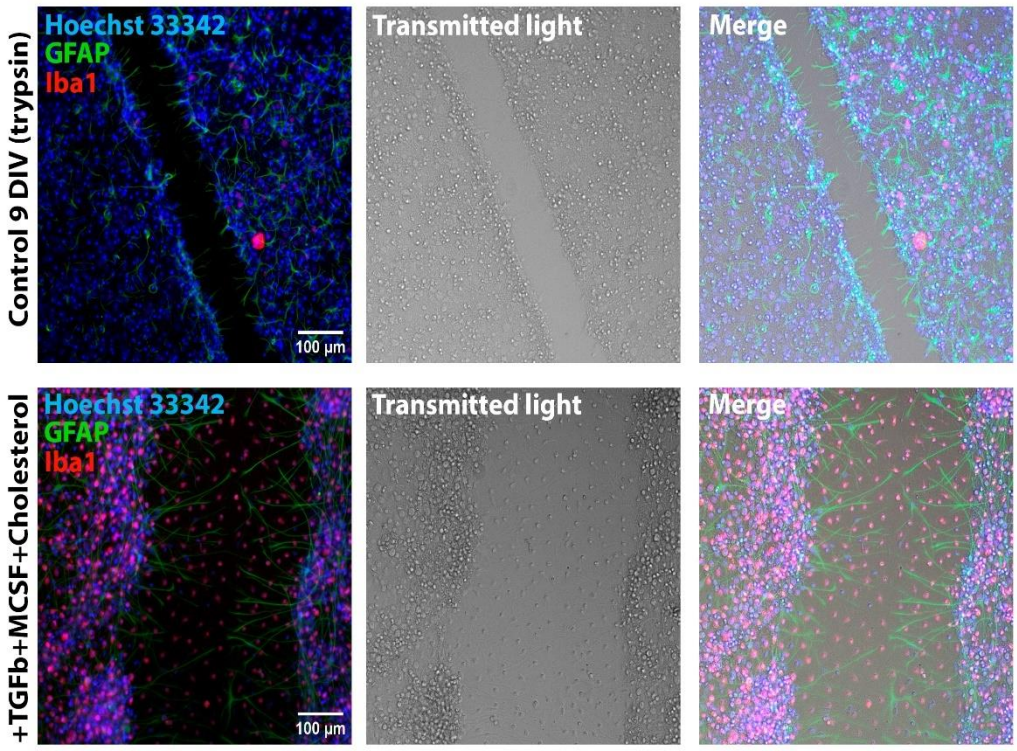

Figure 6. Images of 7 DIV TRY-cultures grown without addition (upper row) and in the presence (lower row) of TGFβ+MCSF+cholesterol two days after scratching. Cultures were stained with antibodies against GFAP and Iba1. The nuclei were stained with Hoechst 33342.

 doi:10.20944/preprints202411.1853.v1

An interesting feature of PAP-cultures, in addition to increasing the amount of microglia compared to TRY-cultures, is the difference in its phenotype, namely in the greater quantity of polarized microglia, as well as in the lesser quantity of amoeboid microglia in the case of culture incubation with TGFb+MCSF+cholesterol, at least on the second day of cultivation. If ameboid microglia is considered to be activated, it can be assumed that papain inhibits induced microglia activation. Similar effects of papain in suppressing proinflammatory signaling cascade activation have been previously demonstrated for other cell types [46–49]. In turn, if bushy microglia, for which more intense CDr20 transformation has been shown, is also considered active [36], but this activation state is probably not polar as in the case of amoeboid microglia, its reduced content in PAP-cultures could also be evidence of papain's inhibitory (anti-inflammatory) action regarding microglial activation, however in this case, the activation is caused by manipulations during culture preparation. Similar astrocyte activation, caused by peculiarities of pure astrocytic culture preparation, has been demonstrated previously by other researchers [9].

5. Conclusions

Thus, it can be concluded that the use of papain as an enzyme for extracellular matrix degradation provides the formation of neuron-glial cultures with developed neuronal and astrocytic networks, as well as with more proliferative microglia compared to cultures prepared using trypsin. Such cultures can be fully considered mixed tricultures in which three major cell populations are present, with microglia in a more natural microenvironment. Unlike co-cultures of microglia and astrocytes or neurons, which involve isolating cultures of separate cell populations and their subsequent mixing [4], used by other researchers and us [10,11] approach makes it possible to simplify in methodological terms the preparation of mixed cultures using biomaterial from one animal while avoiding substantial disproportion in population composition.

The observed differences in the quantity of $Iba1^+$ and $CDr20^+$ microglia in PAP- and TRY-cultures necessitate further evaluation of the reliability of using Iba1 as a microglial marker in mixed cultures. In turn, the demonstrated features of CDr20 transformation dynamics and patterns of calcium responses to ATP in microglial cells of different phenotypes can be used to classify this cell type. Although we showed that the quantity of microglia in PAP-cultures exceeds that in TRY-cultures, the question of microglial maturity in PAP-cultures remains open and is the subject of further separate research. The existing method of assessing microglial maturity by its ability to induce caspase-3-mediated apoptosis when adding lipopolysaccharide (LPS) is rather indirect, considering that the TLR4 receptor, which is the target of LPS, can also be expressed by astrocytes [50,51], and as is known, astrocytes, like microglia, can release various pro- and anti-inflammatory cytokines involved in the implementation of the inflammatory response [52]. For comprehensive determination of microglial maturity, a combination of approaches will be required, including analysis of the expression of a specific set of genes, as well as immunocytochemical staining and morphometric analysis.

Supplementary Materials: The following supporting information can be downloaded at the website of this paper posted on Preprints.org, Figure S1: title; Table S1: title; Video S1: title.

Author Contributions: Conceptualization, S.G.G. and A.M.K.; methodology, S.G.G.; Formal analysis, S.G.G.; Investigation, I.A.T., V.N.M. and S.G.G.; Resources, S.A.M.; Writing—original draft preparation, S.G.G.; Writing—review and editing, V.N.M., A.M.K., S.A.M., I.A.T.; Visualization, S.G.G.; Funding Acquisition, V.N.M. All authors have read and agreed to the published version of the manuscript.

Funding: This research was funded by the Russian Science Foundation (grant no. 23-25-00014).

Institutional Review Board Statement: All animal procedures were approved by the Bioethics Committee of the Institute of Cell Biophysics (ICB) and carried out according to Act708n (23 August 2010) of the Russian Federation National Ministry of Public Health, which states the rules of laboratory practice for the care and use of laboratory animals, and the Council Directive 2010/63 EU of the European Parliament on the protection of animals used for scientific purposes. ICB RAS Animal Facility provided the animals for experiments in accordance with the applications approved by the Commission on Biosafety and Bio-ethics of Institute of Cell Biophysics (Permission No. 4, 14 March 2022; Permission No. 3, 12 March 2023). Pregnant rats were housed 2 to

3 in a cage in the ICB RAS animal facility with 12 12-hour light-dark cycles and access to food and water ad libitum.

Data Availability Statement: The original contributions presented in the study are included in the article supplementary material, further inquiries can be directed to the corresponding authors.

Acknowledgments: The authors sincerely thank the Optical Microscopy and Spectrophotometry core facility of ICB RAS at Federal Research Center "Pushchino Scientific Center for Biological Research of the Russian Academy of Sciences" for technical support.

Conflicts of Interest: The authors declare no conflicts of interest.

References

1. Dadwal, S.; Heneka, M.T. Microglia heterogeneity in health and disease. FEBS Open Bio 2024, 14, 217–229, doi:10.1002/2211-5463.13735.
2. Deus, J.L. de; Faborode, O.S.; Nandi, S. Synaptic Pruning by Microglia: Lessons from Genetic Studies in Mice. Dev. Neurosci. 2024, 1–21, doi:10.1159/000541379.
3. Pesti, I.; Légrádi, Á.; Farkas, E. Primary microglia cell cultures in translational research: Strengths and limitations. J. Biotechnol. 2024, 386, 10–18, doi:10.1016/j.jbiotec.2024.03.005.
4. Aktories, P.; Petry, P.; Kierdorf, K. Microglia in a Dish-Which Techniques Are on the Menu for Functional Studies? Front. Cell. Neurosci. 2022, 16, 908315, doi:10.3389/fncel.2022.908315.
5. Roqué, P.J.; Costa, L.G. Co-Culture of Neurons and Microglia. Curr. Protoc. Toxicol. 2017, 74, 11.24.1-11.24.17, doi:10.1002/cptx.32.
6. Dessi, F.; Pollard, H.; Moreau, J.; Ben-Ari, Y.; Charriaut-Marlangue, C. Cytosine arabinoside induces apoptosis in cerebellar neurons in culture. J. Neurochem. 1995, 64, 1980–1987, doi:10.1046/j.1471-4159.1995.64051980.x.
7. Besirli, C.G.; Deckwerth, T.L.; Crowder, R.J.; Freeman, R.S.; Johnson, E.M. Cytosine arabinoside rapidly activates Bax-dependent apoptosis and a delayed Bax-independent death pathway in sympathetic neurons. Cell Death Differ. 2003, 10, 1045–1058, doi:10.1038/sj.cdd.4401259.
8. Nakayama, S.; Adachi, M.; Hatano, M.; Inahata, N.; Nagao, T.; Fukushima, N. Cytosine arabinoside induces phosphorylation of histone H2AX in hippocampal neurons via a noncanonical pathway. Neurochem. Int. 2021, 142, 104933, doi:10.1016/j.neuint.2020.104933.
9. Du Fang; Li, Z.; Zhong-ming, Q.; Mei, W.X.; Ho, Y.W.; Yuan, X.W.; Ya, K. Expression of bystin in reactive astrocytes induced by ischemia/reperfusion and chemical hypoxia in vitro. Biochim. Biophys. Acta 2008, 1782, 658–663, doi:10.1016/j.bbadis.2008.09.007.
10. Goshi, N.; Morgan, R.K.; Lein, P.J.; Seker, E. A primary neural cell culture model to study neuron, astrocyte, and microglia interactions in neuroinflammation. J. Neuroinflammation 2020, 17, 155, doi:10.1186/s12974-020-01819-z.
11. Goshi, N.; Kim, H.; Seker, E. Primary Cortical Cell Tri-Culture-Based Screening of Neuroinflammatory Response in Toll-like Receptor Activation. Biomedicines 2022, 10, doi:10.3390/biomedicines10092122.
12. Kim, H.; Le, B.; Goshi, N.; Zhu, K.; Grodzki, A.C.; Lein, P.J.; Zhao, M.; Seker, E. Primary cortical cell tri-culture to study effects of amyloid-β on microglia function and neuroinflammatory response. J. Alzheimers. Dis. 2024, 13872877241291142, doi:10.1177/13872877241291142.
13. Woolf, Z.; Stevenson, T.J.; Lee, K.; Jung, Y.; Park, T.I.H.; Curtis, M.A.; Montgomery, J.M.; Dragunow, M. Isolation of adult mouse microglia using their in vitro adherent properties. STAR Protoc. 2021, 2, 100518, doi:10.1016/j.xpro.2021.100518.
14. Brewer, G.J. Isolation and culture of adult rat hippocampal neurons. J. Neurosci. Methods 1997, 71, 143–155, doi:10.1016/s0165-0270(96)00136-7.
15. Hu, C.-Y.; Du, R.-L.; Xiao, Q.-X.; Geng, M.-J. Differences between cultured cortical neurons by trypsin and papain digestion. Ibrain 2022, 8, 93–99, doi:10.1002/ibra.12028.
16. Gaidin, S.G.; Zinchenko, V.P.; Sergeev, A.I.; Teplov, I.Y.; Mal'tseva, V.N.; Kosenkov, A.M. Activation of alpha-2 adrenergic receptors stimulates GABA release by astrocytes. Glia 2020, 68, 1114–1130, doi:10.1002/glia.23763.
17. Laryushkin, D.P.; Maiorov, S.A.; Zinchenko, V.P.; Gaidin, S.G.; Kosenkov, A.M. Role of L-Type Voltage-Gated Calcium Channels in Epileptiform Activity of Neurons. Int. J. Mol. Sci. 2021, 22, doi:10.3390/ijms221910342.
18. Zinchenko, V.P.; Kosenkov, A.M.; Gaidin, S.G.; Sergeev, A.I.; Dolgacheva, L.P.; Tuleukhanov, S.T. Properties of GABAergic Neurons Containing Calcium-Permeable Kainate and AMPA-Receptors. Life (Basel) 2021, 11, doi:10.3390/life11121309.
19. Gaidin, S.G.; Maiorov, S.A.; Laryushkin, D.P.; Zinchenko, V.P.; Kosenkov, A.M. A novel approach for vital visualization and studying of neurons containing Ca2+ -permeable AMPA receptors. J. Neurochem. 2023, 164, 583–597, doi:10.1111/jnc.15729.

20. Laryushkin, D.P.; Maiorov, S.A.; Zinchenko, V.P.; Mal'tseva, V.N.; Gaidin, S.G.; Kosenkov, A.M. Of the Mechanisms of Paroxysmal Depolarization Shifts: Generation and Maintenance of Bicuculline-Induced Paroxysmal Activity in Rat Hippocampal Cell Cultures. Int. J. Mol. Sci. 2023, 24, doi:10.3390/ijms241310991.
21. Zinchenko, V.P.; Teplov, I.Y.; Kosenkov, A.M.; Gaidin, S.G.; Kairat, B.K.; Tuleukhanov, S.T. Participation of calcium-permeable AMPA receptors in the regulation of epileptiform activity of hippocampal neurons. Front. Synaptic Neurosci. 2024, 16, 1349984, doi:10.3389/fnsyn.2024.1349984.
22. Kim, B.; Fukuda, M.; Lee, J.-Y.; Su, D.; Sanu, S.; Silvin, A.; Khoo, A.T.T.; Kwon, T.; Liu, X.; Chi, W.; et al. Visualizing Microglia with a Fluorescence Turn-On Ugt1a7c Substrate. Angew. Chem. Int. Ed Engl. 2019, 58, 7972–7976, doi:10.1002/anie.201903058".
23. Hol, E.M.; Pekny, M. Glial fibrillary acidic protein (GFAP) and the astrocyte intermediate filament system in diseases of the central nervous system. Curr. Opin. Cell Biol. 2015, 32, 121–130, doi:10.1016/j.ceb.2015.02.004.
24. Burnstock, G.; Knight, G.E. Cellular distribution and functions of P2 receptor subtypes in different systems. Int. Rev. Cytol. 2004, 240, 31–304, doi:10.1016/S0074-7696(04)40002-3.
25. Del Puerto, A.; Wandosell, F.; Garrido, J.J. Neuronal and glial purinergic receptors functions in neuron development and brain disease. Front. Cell. Neurosci. 2013, 7, 197, doi:10.3389/fncel.2013.00197.
26. Xing, S.; Grol, M.W.; Grutter, P.H.; Dixon, S.J.; Komarova, S.V. Modeling Interactions among Individual P2 Receptors to Explain Complex Response Patterns over a Wide Range of ATP Concentrations. Front. Physiol. 2016, 7, 294, doi:10.3389/fphys.2016.00294.
27. Di Garbo, A.; Barbi, M.; Chillemi, S.; Alloisio, S.; Nobile, M. Calcium signalling in astrocytes and modulation of neural activity. Biosystems. 2007, 89, 74–83, doi:10.1016/j.biosystems.2006.05.013.
28. Kleinsimlinghaus, K.; Marx, R.; Serdar, M.; Bendix, I.; Dietzel, I.D. Strategies for repair of white matter: Influence of osmolarity and microglia on proliferation and apoptosis of oligodendrocyte precursor cells in different basal culture media. Front. Cell. Neurosci. 2013, 7, 277, doi:10.3389/fncel.2013.00277.
29. Yang, S.; Wu, J.; Xian, X.; Chen, Q. Isolation, culture, and characterization of duck primary neurons. Poult. Sci. 2023, 102, 102485, doi:10.1016/j.psj.2023.102485.
30. Mueller-Buehl, C.; Wegrzyn, D.; Bauch, J.; Faissner, A. Regulation of the E/I-balance by the neural matrisome. Front. Mol. Neurosci. 2023, 16, 1102334, doi:10.3389/fnmol.2023.1102334.
31. Vigneault, É.; Poirel, O.; Riad, M.; Prud'homme, J.; Dumas, S.; Turecki, G.; Fasano, C.; Mechawar, N.; El Mestikawy, S. Distribution of vesicular glutamate transporters in the human brain. Front. Neuroanat. 2015, 9, 23, doi:10.3389/fnana.2015.00023.
32. Chaudhry, F.A.; Reimer, R.J.; Bellocchio, E.E.; Danbolt, N.C.; Osen, K.K.; Edwards, R.H.; Storm-Mathisen, J. The vesicular GABA transporter, VGAT, localizes to synaptic vesicles in sets of glycinergic as well as GABAergic neurons. J. Neurosci. 1998, 18, 9733–9750, doi:10.1523/JNEUROSCI.18-23-09733.1998.
33. He, Y.; Taylor, N.; Yao, X.; Bhattacharya, A. Mouse primary microglia respond differently to LPS and poly(I:C) in vitro. Sci. Rep. 2021, 11, 10447, doi:10.1038/s41598-021-89777-1.
34. Cuní-López, C.; Stewart, R.; Quek, H.; White, A.R. Recent Advances in Microglia Modelling to Address Translational Outcomes in Neurodegenerative Diseases. Cells 2022, 11, doi:10.3390/cells11101662.
35. Lier, J.; Streit, W.J.; Bechmann, I. Beyond Activation: Characterizing Microglial Functional Phenotypes. Cells 2021, 10, doi:10.3390/cells10092236.
36. Green, T.R.F.; Rowe, R.K. Quantifying microglial morphology: An insight into function. Clin. Exp. Immunol. 2024, 216, 221–229, doi:10.1093/cei/uxae023.
37. Lier, J.; Winter, K.; Bleher, J.; Grammig, J.; Mueller, W.C.; Streit, W.; Bechmann, I. Loss of IBA1-Expression in brains from individuals with obesity and hepatic dysfunction. Brain Res. 2019, 1710, 220–229, doi:10.1016/j.brainres.2019.01.006.
38. Waller, R.; Baxter, L.; Fillingham, D.J.; Coelho, S.; Pozo, J.M.; Mozumder, M.; Frangi, A.F.; Ince, P.G.; Simpson, J.E.; Highley, J.R. Iba-1-/CD68+ microglia are a prominent feature of age-associated deep subcortical white matter lesions. PLoS One 2019, 14, e0210888, doi:10.1371/journal.pone.0210888.
39. Fritze, J.; Muralidharan, C.; Stamp, E.; Ahlenius, H. Microglia undergo disease-associated transcriptional activation and CX3C motif chemokine receptor 1 expression regulates neurogenesis in the aged brain. Dev. Neurobiol. 2024, 84, 128–141, doi:10.1002/dneu.22939.
40. Jurga, A.M.; Paleczna, M.; Kuter, K.Z. Overview of General and Discriminating Markers of Differential Microglia Phenotypes. Front. Cell. Neurosci. 2020, 14, 198, doi:10.3389/fncel.2020.00198.
41. Kim, W.; Kim, M.; Kim, B. Unraveling the enigma: Housekeeping gene Ugt1a7c as a universal biomarker for microglia. Front. Psychiatry 2024, 15, 1364201, doi:10.3389/fpsyt.2024.1364201.
42. Kenkhuis, B.; Somarakis, A.; Kleindouwel, L.R.T.; van Roon-Mom, W.M.C.; Höllt, T.; van der Weerd, L. Co-expression patterns of microglia markers Iba1, TMEM119 and P2RY12 in Alzheimer's disease. Neurobiol. Dis. 2022, 167, 105684, doi:10.1016/j.nbd.2022.105684.
43. Hoffmann, A.; Kann, O.; Ohlemeyer, C.; Hanisch, U.-K.; Kettenmann, H. Elevation of basal intracellular calcium as a central element in the activation of brain macrophages (microglia): Suppression of receptor-

 doi:10.20944/preprints202411.1853.v1

evoked calcium signaling and control of release function. J. Neurosci. 2003, 23, 4410–4419, doi:10.1523/JNEUROSCI.23-11-04410.2003.
44. Palomba, N.P.; Martinello, K.; Cocozza, G.; Casciato, S.; Mascia, A.; Di Gennaro, G.; Morace, R.; Esposito, V.; Wulff, H.; Limatola, C.; et al. ATP-evoked intracellular Ca2+ transients shape the ionic permeability of human microglia from epileptic temporal cortex. J. Neuroinflammation 2021, 18, 44, doi:10.1186/s12974-021-02096-0.
45. Beaino, W.; Janssen, B.; Kooij, G.; van der Pol, S.M.A.; van Het Hof, B.; van Horssen, J.; Windhorst, A.D.; Vries, H.E. de. Purinergic receptors P2Y12R and P2X7R: Potential targets for PET imaging of microglia phenotypes in multiple sclerosis. J. Neuroinflammation 2017, 14, 259, doi:10.1186/s12974-017-1034-z.
46. Fei, X.; Yuan, W.; Zhao, Y.; Wang, H.; Bai, S.; Huang, Q. Papain Ameliorates the MPAs Formation-Mediated Activation of Monocytes by Inhibiting Cox-2 Expression via Regulating the MAPKs and PI3K/Akt Signal Pathway. Biomed Res. Int. 2018, 2018, 3632084, doi:10.1155/2018/3632084.
47. Kang, Y.-M.; Kang, H.-A.; Cominguez, D.C.; Kim, S.-H.; An, H.-J. Papain Ameliorates Lipid Accumulation and Inflammation in High-Fat Diet-Induced Obesity Mice and 3T3-L1 Adipocytes via AMPK Activation. Int. J. Mol. Sci. 2021, 22, doi:10.3390/ijms22189885.
48. Jiang, L.; Xu, C.; Zhao, Y.; Huang, Q.; Yuan, W.; Wu, Y.; Fei, X. Papain ameliorates monocyte-platelet aggregate formation-mediated inflammatory responses in monocytes by upregulating miRNA-146a transcription. PLoS One 2022, 17, e0278059, doi:10.1371/journal.pone.0278059.
49. Kim, H.-M.; Kang, Y.-M.; Lee, M.; An, H.-J. Papain Suppresses Atopic Skin Inflammation through Anti-Inflammatory Activities Using In Vitro and In Vivo Models. Antioxidants (Basel) 2024, 13, doi:10.3390/antiox13080928.
50. Gorina, R.; Font-Nieves, M.; Márquez-Kisinousky, L.; Santalucia, T.; Planas, A.M. Astrocyte TLR4 activation induces a proinflammatory environment through the interplay between MyD88-dependent NFκB signaling, MAPK, and Jak1/Stat1 pathways. Glia 2011, 59, 242–255, doi:10.1002/glia.21094.
51. Li, L.; Acioglu, C.; Heary, R.F.; Elkabes, S. Role of astroglial toll-like receptors (TLRs) in central nervous system infections, injury and neurodegenerative diseases. Brain Behav. Immun. 2021, 91, 740–755, doi:10.1016/j.bbi.2020.10.007.
52. Linnerbauer, M.; Wheeler, M.A.; Quintana, F.J. Astrocyte Crosstalk in CNS Inflammation. Neuron 2020, 108, 608–622, doi:10.1016/j.neuron.2020.08.012.